ORIGINAL ARTICLE

Cancer Science WILEY

Glycosylation of MUC6 by α1,4-linked N-acetylglucosamine enhances suppression of pancreatic cancer malignancy

Atsuko Yuki[1] | Chifumi Fujii[1,2] | Kazuhiro Yamanoi[1,3] | Hisanori Matoba[1] | Satoru Harumiya[1] | Masatomo Kawakubo[1] | Jun Nakayama[1]

[1]Department of Molecular Pathology, Shinshu University School of Medicine, Matsumoto, Japan

[2]Department of Biotechnology, Interdisciplinary Cluster for Cutting Edge Research, Institute for Biomedical Sciences, Shinshu University, Matsumoto, Japan

[3]Department of Pathology, Keio University School of Medicine, Tokyo, Japan

Correspondence
Chifumi Fujii, Department of Molecular Pathology, Shinshu University School of Medicine, and Department of Biotechnology, Interdisciplinary Cluster for Cutting Edge Research, Institute for Biomedical Sciences, Shinshu University, 3-1-1 Asahi, Matsumoto 390-8621, Japan.
Email: chifumif@shinshu-u.ac.jp

Abstract

Biomarkers for early diagnosis of pancreatic cancer are greatly needed, as the high fatality of this cancer is in part due to delayed detection. α1,4-linked N-acetylglucosamine (αGlcNAc), a unique O-glycan specific to gastric gland mucus, is biosynthesized by α1,4-N-acetylglucosaminyltransferase (α4GnT) and primarily bound at the terminal glycosylated residue to scaffold protein MUC6. We previously reported that αGlcNAc expression decreases at early stages of neoplastic pancreatic lesions, followed by decreased MUC6 expression, although functional effects of these outcomes were unknown. Here, we ectopically expressed α4GnT, the αGlcNAc biosynthetic enzyme, together with MUC6 in the human pancreatic cancer cell lines MIA PaCa-2 and PANC-1, neither of which expresses α4GnT and MUC6. We observed significantly suppressed proliferation in both lines following coexpression of α4GnT and MUC6. Moreover, cellular motility decreased following MUC6 ectopic expression, an effect enhanced by cotransduction with α4GnT. MUC6 expression also attenuated invasiveness of both lines relative to controls, and this effect was also enhanced by additional α4GnT expression. We found αGlcNAc-bound MUC6 formed a complex with trefoil factor 2. Furthermore, analysis of survival curves of patients with pancreatic ductal adenocarcinoma using a gene expression database showed that samples marked by higher *A4GNT* or *MUC6* mRNA levels were associated with relatively favorable prognosis. These results strongly suggest that αGlcNAc and MUC6 function as tumor suppressors in pancreatic cancer and that decreased expression of both may serve as a biomarker of tumor progression to pancreatic cancer.

KEYWORDS
malignant phenotype, MUC6, pancreatic cancer, α4GnT, αGlcNAc

Atsuko Yuki and Chifumi Fujii contributed equally to this work.

1 | INTRODUCTION

In 2020, the number of deaths from pancreatic cancer was almost comparable to the number of cases, namely, 466 003 deaths versus 495 773 cases, making it the seventh leading cause of cancer death in both men and women worldwide.[1] Despite advances in diagnostic tools, including various imaging modalities and echo-guided fine-needle aspiration biopsy, early diagnosis, which could lead to effective treatment, remains difficult, leading to poor prognosis. Therefore, novel biomarkers with specificity for precursor pancreatic cancer lesions are greatly needed.

Aberrant expression of gastric-type mucin in the pancreatic epithelium is an important process in the early stages of pancreatic tumor progression.[2-7] Mucins secreted from the gastroduodenal mucosa are classified into surface mucins and gland mucins,[8] which contain MUC5AC and MUC6, respectively.[9] Gland mucin characteristically contains unique O-linked oligosaccharides (O-glycans) exhibiting terminal α1,4-linked N-acetylglucosamine residues (αGlcNAc) which are primarily bound to scaffold protein MUC6.[10-12] In normal gastric mucosa, αGlcNAc and MUC6 are coexpressed in gland mucous cells such as pyloric glands and mucous neck cells.[11] Previously, we used expression cloning to identify α1,4-N-acetylglucosaminyltransferase (α4GnT), which catalyzes αGlcNAc biosynthesis.[13] When we generated mice deficient in $A4gnt$, which encodes α4GnT, αGlcNAc gland mucin was completely lost and mice spontaneously developed differentiated gastric adenocarcinoma.[14] Moreover, our previous analyses of αGlcNAc and MUC6 expression in human gastric lesions suggested that αGlcNAc might suppress development of malignancy.[15-18] Furthermore, various studies of αGlcNAc and MUC6 expression in gastric mucin-producing tumors arising in extra gastric organs, such as Barrett's esophagus,[18,19] pancreas,[18,20] uterine cervix,[21,22] biliary tract[23] and ovary,[24] suggest that αGlcNAc may inhibit development of malignancy in those contexts.[18-24]

In normal human pancreas, αGlcNAc and MUC6 are coexpressed in accessory gland mucous cells of the pancreaticobiliary tract.[11] Others have reported that αGlcNAc is expressed in intraductal papillary mucinous neoplasia (IPMN)[6,25] and pancreatic intraepithelial neoplasia (PanIN).[6] Previously, we evaluated expression patterns of the gastric mucin markers MUC5AC, MUC6, and αGlcNAc in pancreatic precursor lesions and invasive carcinomas by immunohistochemistry.[20] We found that in both PanIN–invasive ductal adenocarcinoma of the pancreas (IDAC) and IPMN–IPMN with associated invasive carcinoma (IPMNAIC) sequences, αGlcNAc expression levels relative to MUC6 begin to decrease early in tumor progression, and then MUC6 expression subsequently decreases or is lost.[20] On the other hand, we observed no changes in MUC5AC expression throughout disease stages.[20] Others have reported higher MUC6 expression in IPMN than in IDAC and that MUC6 expression is an early event in PanIN,[6] and MUC6 overexpression occurs early in development of pancreatic adenocarcinoma.[3,7] These studies suggest that reduced levels of αGlcNAc and MUC6 may serve as useful biomarkers in early diagnosis of pancreatic cancer. However, direct effects of αGlcNAc and MUC6 on malignant phenotypes of pancreatic cancer cells have been elusive.

Here, we ectopically expressed α4GnT and MUC6 in the human pancreatic cancer cell lines MIA PaCa-2 and PANC-1, neither of which expresses α4GnT or MUC6, and assessed phenotypes associated with malignancy. We also investigated whether $A4GNT$ or $MUC6$ mRNA expression levels are associated with prognosis of pancreatic ductal adenocarcinoma patients using the GEO database.

2 | MATERIALS AND METHODS

2.1 | Antibodies and reagents

Anti-Myc-tag antibody (clone My3, mouse IgG2) was purchased from MBL. Antibodies against MUC6 (clone CLH5, mouse IgG), β-actin (clone C4, mouse IgG), and normal mouse IgG were purchased from Santa Cruz. Anti-αGlcNAc (clone HIK1083, mouse IgM) was purchased from Kantokagaku. Rabbit polyclonal antibodies against α4GnT[11] and core 2 β-1,6-N-acetylglucosaminyltransferase (C2GnT)[26] were prepared as described previously. Anti-trefoil factor 2 (TFF2), rabbit polyclonal antibodies, was purchased from Proteintech.

2.2 | Cell culture

The human pancreatic cancer cell line MIA PaCa-2 was obtained from JCRB Cell Bank (Osaka, Japan), and the human pancreatic ductal carcinoma cell line PANC-1 was obtained from the RIKEN BRC Cell Bank. MIA PaCa-2 or PANC-1 was maintained in DMEM/high glucose (FUJIFILM Wako) or RPMI-1640 (FUJIFILM Wako), respectively, supplemented with 10% heat-inactivated fetal bovine serum (FBS; Hyclone) and penicillin/streptomycin (FUJIFILM Wako) at 37°C in a humidified 5% CO_2 atmosphere. The retroviral packaging cell line, 293T (ATCC), was maintained in DMEM/high glucose containing 10% FBS at 37°C in a 5% CO_2 humidified atmosphere.

2.3 | Establishment of α4GnT- and/or MUC6-expressing cells

The human $A4GNT$ open reading frame (ORF) was PCR-amplified from pcDNA I containing full-length $A4GNT$ cDNA[13] as template with primers flanked by an EcoRI site on the 5' end and an XhoI site on the 3' end. The amplicon was inserted into the EcoRI-XhoI site of the pMXs-IRES-Puro retroviral vector (Cell Biolabs). The human $MUC6$ ORF was excised from the TrueClone ORF Collection MUC6 (RC219711; OriGene Technologies) and subcloned into the pMXs-IRES-Bsd retroviral vector (Cell biolabs) by inserting an in-flame C-terminal Myc-tag sequence. Empty vectors served as negative controls. 293T cells cultured in DMEM/high glucose containing 10% FBS and 4 mM L-glutamine

(FUJIFILM Wako) were incubated with recombinant retroviral vectors, VSV-G inserted plasmid (Add gene), gag/pol carrying plasmid (Add gene), and Linear polyethyleneimine MAX (Polysciences, Inc) for 6-8 hours at 37°C 5% CO_2. Thereafter, cells were cultured in fresh medium. Supernatants containing retroviral particles were harvested 2-3 days post transfection, filtered through a 0.45-μm filter, concentrated by centrifugation at 8000 g for 16 hours, and used to infect target cells. Concentrated virus supernatant carrying *MUC6* or control virus was added to 12-well plates coated with 50 μg/mL RetroNectin (Takara Bio), which were centrifuged at 1080 g for 4 hours at 32°C. The viral supernatants were then removed, and MIA PaCa-2 or PANC-1 cells (2×10^4 cells per well) were seeded and incubated at 37°C for 24 hours. Then, *MUC6*-transduced MIA PaCa-2 or PANC-1 cells were infected with retrovirus carrying *A4GNT* or control virus using the procedure described above and incubated for 48 hours at 37°C. Infected MIA PaCa-2 cells were subcultured in fresh DMEM/high glucose containing 5 μg/mL puromycin (FUJIFILM Wako) and 20 μg/mL blasticidin (FUJIFILM Wako). Infected PANC-1 cells were subcultured in fresh RPMI-1640 containing 5 μg/mL puromycin/40 μg/mL blasticidin. Puromycin- and blasticidin-resistant cell pools were readily established within 10 days. Three kinds of cells were generated from each line; *MUC6*-transduced MIA PaCa-2-MUC6 or PANC-1-MUC6 cells, *A4GNT/MUC6*-transduced MIA PaCa-2-MUC6/A4GNT or PANC-1-MUC6/A4GNT cells, and control MIA PaCa-2-Control or PANC-1-Control cells.

2.4 | Immunoprecipitation and Western blotting

Cultured cells to be analyzed were harvested, sonicated, and homogenized in immunoprecipitation (IP) buffer (50 mmol/L Tris-HCl [pH 8.0], 150 mmol/L NaCl, 1 mmol/L $MgCl_2$, 0.5% Nonidet P-40, 10 mmol/L NaF, 1 mmol/L Na_3VO_4, 1 mmol/L phenylmethylsulfonylfluoride, and 1 unit of complete protease inhibitor cocktail EDTA-free [Roche]). Protein concentrations in whole-cell lysates (WCLs) were determined using a BCA protein assay (Thermo Fisher Scientific). WCL proteins were incubated with anti-Myc-tag antibody with gentle rocking overnight at 4°C. Products were then incubated with protein G Sepharose (GE Healthcare) for an additional 1 hour at 4°C. For IP of culture supernatant, confluent cells were cultured in the serum-free medium for 48 hours, and supernatant was incubated with anti-Myc-tag antibody or normal mouse IgG overnight followed by incubation with Dynabeads Protein G (Veritas) for 1 hour. Beads were then washed with IP buffer or PBS three times and heated to 98°C for 5 minutes in Laemmli sample buffer (50 mmol/L Tris-HCl [pH 6.8], 2.5% SDS, 2.5% 2-mercaptoethanol, 0.005% bromophenol blue, and 5% glycerol). Protein samples were separated by SDS-PAGE and electrophoretically transferred to PVDF membranes, which were blocked for 1 hour with 5% nonfat dry milk in TBS buffer (50 mmol/L Tris-HCl [pH 7.5] and 150 mmol/L NaCl) at room temperature and

thereafter incubated with primary antibodies overnight at 4°C. After incubation, membranes were washed in TBS containing 0.01% Tween 20 three times and incubated at room temperature for 1 hour with horseradish peroxidase (HRP)–conjugated secondary antibodies (DAKO). For anti-αGlcNAc, HRP–conjugated anti-mouse IgM (Jackson ImmunoResearch) was used as the secondary antibody. Detection was carried out using the enhanced chemiluminescence detection system Immobilon Western chemiluminescent HRP substrate (Merck Millipore). All data were processed and analyzed using Cool Saver AE-6955 (ATTO) and CS Analyzer software (ATTO).

2.5 | Cell proliferation analysis

We used 96-well tissue culture plates to assess anchorage-dependent cell proliferation and 96-well plates coated with poly-(2-hydroxymethyl methacrylate) (poly-HEMA) (Sigma) to analyze anchorage-independent cell proliferation. For both, 1×10^3 cells were seeded in each 96-well plate and 0, 24, 48, and 72 hours later CellTiter96®AQueousOneSolution (MTS solution; Promega) was added. Two hours later, color density was measured at 490 nm using a microplate reader (Dainippon Pharmaceutical).

2.6 | Transwell migration assay

MIA PaCa-2 cells (5×10^4) in serum-free DMEM/high glucose or PANC-1 cells (7.5×10^4) in serum-free RPMI-1640 were seeded on the top of Transwell inserts with an 8.0-μm-pore-size membrane (BD Falcon). The bottom chamber contained DMEM/high glucose or RPMI-1640 with 10% FBS, respectively, as chemoattractant. After incubation for 24 (MIA PaCa-2) or 6 (PANC-1) hours, cells on the upper membrane surface were removed with a cotton swab. MIA PaCa-2 cells that had migrated to the lower surface of the membranes were fixed with 70% ethanol and then treated with methanol. PANC-1 cells that had migrated to the lower surface were fixed with methanol, and both were stained with 0.2% crystal violet. Migrated cells were observed by light microscopy (×200 magnification) and counted in five randomly selected fields from triplicate wells.

2.7 | Matrigel invasion assay

Transwell cell culture inserts (membrane pore size: 8.0 μm; BD Falcon) were coated with 25 μg or 50 μg Matrigel (BD Biosciences), respectively, to analyze MIA PaCa-2 or PANC-1 cells. One hundred thousand each of MIA PaCa-2 cells in serum-free DMEM/high glucose or PANC-1 cells in serum-free RPMI-1640 were seeded in the upper chamber of inserts. The lower chamber contained DMEM/high glucose or RPMI-1640, respectively, with 10% FBS as chemoattractant. After a 24-hour incubation, cells were fixed, stained, and

analyzed using the procedure described in the section "Transwell migration assay."

2.8 | Prognostic analysis using a database

An online database was utilized to evaluate potential correlation between *A4GNT* or *MUC6* expression and prognosis of pancreatic ductal adenocarcinoma patients. The GSE dataset (GSE28735) was downloaded from the NCBI Gene Expression Omnibus (GEO) database (https://www.ncbi.nlm.nih.gov/geo/). This dataset contains cDNA microarray gene-expression profiles of pancreatic tumors and adjacent nontumor tissues from pancreatic ductal adenocarcinoma patients. For this study, we used only tumor tissue data. *A4GNT* or *MUC6* expression levels were normalized to *GAPDH,* and the relationship to prognosis was analyzed using the Kaplan-Meier Plotter (https://kmplot.com/analysis/).

2.9 | Statistical analysis

Statistical analysis for cellular experiments was performed using EZR 1.37[27] (Saitama Medical Center, Jichi Medical University), a graphical user interface for R version 3.4.1 (The R Foundation for Statistical Computing). We used the Kruskal-Wallis test with Holm-corrected Mann-Whitney post hoc tests for cellular experiments. Results were expressed as the mean $\pm$ SD. P-values < .05 were considered statistically significant. Prognosis was analyzed using the Kaplan-Meier Plotter. Hazard ratio (HR) and P-values by log-rank test were determined and displayed.

3 | RESULTS

3.1 | Immunoprecipitation analysis of αGlcNAc-binding MUC6

To establish pancreatic cancer cell lines ectopically expressing MUC6 or MUC6/α4GnT, we used retroviral transduction of the pancreatic cancer cell line MIA PaCa-2 and the pancreatic ductal carcinoma cell line PANC-1 with either MUC6 alone or MUC6 plus α4GnT. We first assessed α4GnT expression in WCLs from transduced MIA PaCa-2-MUC6/A4GNT or PANC-1-MUC6/A4GNT lines by Western blotting and detected a primary band at ~48 kDa representing unglycosylated α4GnT and a minor band at ~63 kDa representing glycosylated α4GnT in both (Figure 1, α4GnT panel of WCL), consistent with our previous analysis of gastric adenocarcinoma AGS cells.[11] Comparable analysis with an anti-MUC6 antibody of WCLs from cells either singly (MUC6) or doubly (MUC6/A4GNT) transduced confirmed MUC6 expression in MIA PaCa-2-MUC6, PANC-1-MUC6, MIA PaCa-2-MUC6/A4GNT, and PANC-1-MUC6/A4GNT cells (Figure 1, MUC6 panel of WCL). As MUC6 constructs were C-terminally Myc tagged, we undertook a similar analysis using
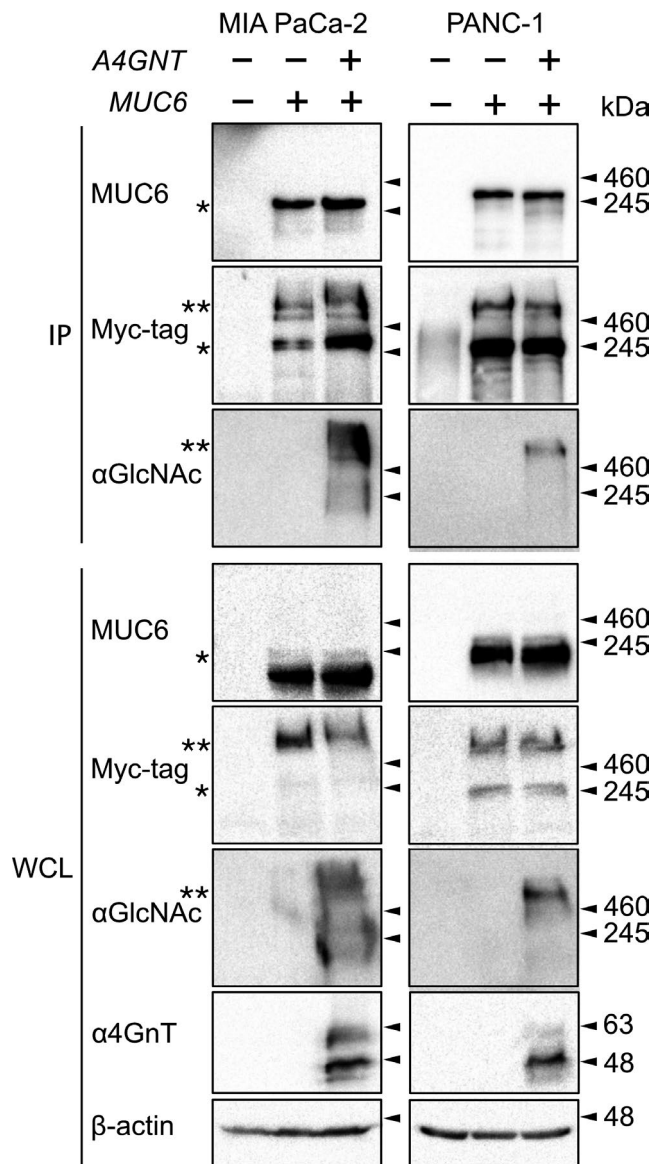
FIGURE 1 Immunoprecipitation (IP) and Western blotting analysis of αGlcNAc, α4GnT, and MUC6 expression. Whole-cell lysates (WCL; bottom five rows) and IP products (top three rows) from MIA PaCa-2 or PANC-1 cells transduced with *MUC6, MUC6/A4GNT,* or control, as indicated, were immunoblotted with antibodies shown on the left side of the figure. *, unglycosylated MUC6; **, glycosylated MUC6. β-actin serves as the loading control

an anti-Myc-tag antibody and detected two bands in all samples: one at ~245 kDa (comparable to the anti-MUC6 antibody) and the other at >460 kDa (Figure 1, Myc-tag panel of WCL). Given that the anti-MUC6 antibody utilized here cannot detect glycosylated MUC6,[24,28] we conclude that >460-kDa bands represented glycosylated MUC6. As confirmation, we performed an IP of WCLs with the anti-Myc-tag antibody followed by immunoblotting with the anti-αGlcNAc antibody. That analysis conducted in both MIA PaCa-2-MUC6/A4GNT and PANC-1-MUC6/A4GNT cells revealed that the >460-kDa band immunoprecipitated with the anti-Myc-tag antibody was positive for

anti-αGlcNAc antibody (Figure 1, αGlcNAc panel of IP), suggesting that it represents MUC6 glycosylated with αGlcNAc. Collectively, these results indicate that transduced gene products are both expressed and post-transcriptionally modified as expected.

## 3.2 | Ectopic MUC6 and α4GnT expression alters cell proliferation in vitro

To investigate the effects of MUC6 or MUC6/α4GnT expression on malignancy, we first analyzed the proliferation of MIA PaCa-2 or PANC-1 cells in vitro. Ectopic expression of MUC6 alone significantly decreased anchorage-dependent cell proliferation of MIA PaCa-2-MUC6 cells, and that rate was further significantly decreased in doubly transduced MIA PaCa-2-MUC6/A4GNT cells (Figure 2A). In PANC-1 cells, expression of both MUC6 and α4GnT also attenuated anchorage-dependent cell proliferation relative to the PANC-1-Control cells and singly transduced PANC-1-MUC6 cells (Figure 2B). Anchorage-independent proliferation was significantly lower in MIA PaCa-2-MUC6 and MIA PaCa-2-MUC6/A4GNT cells compared with MIA PaCa-2-Control cells (Figure 2C). In contrast, anchorage-independent proliferation was comparable in control,

MUC6-transduced, and MUC6/α4GnT-transduced PANC-1 cells (Figure 2D). These results suggest that ectopic expression of MUC6 and α4GnT suppresses anchorage-dependent cell proliferations in MIA PaCa-2 and PANC-1 cells. On the contrary, somewhat different mechanisms may drive anchorage-independent proliferation in those two cancer cell lines.

3.3 | Ectopic MUC6 and α4GnT expression attenuates cell motility

We next examined effects of MUC6 and α4GnT expression on motility of both lines using a Transwell migration assay. We observed significantly decreased migration of MIA PaCa-2-MUC6 relative to MIA PaCa-2-Control cells, and that effect was further significantly reduced in doubly transduced MIA PaCa-2-MUC6/A4GNT cells (Figure 3A, B). Similarly, PANC-1 cell migration was significantly suppressed relative to controls by ectopic MUC6 expression and further significantly attenuated in cells doubly transduced with MUC6 and α4GnT (Figure 3A, C). These results suggest that in both MIA PaCa-2 and PANC-1 cells, ectopic MUC6 expression decreases motility and that MUC6 decorated with αGlcNAc has a more potent effect.

Anchorage-dependent cell proliferation
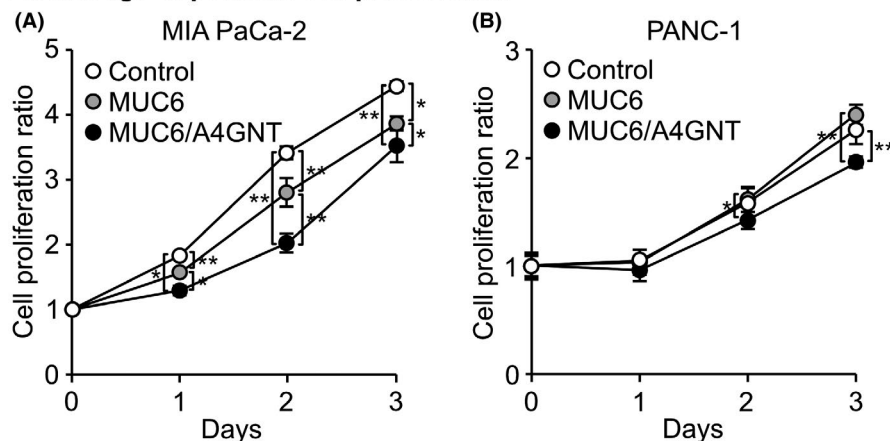
Anchorage-independent cell proliferation
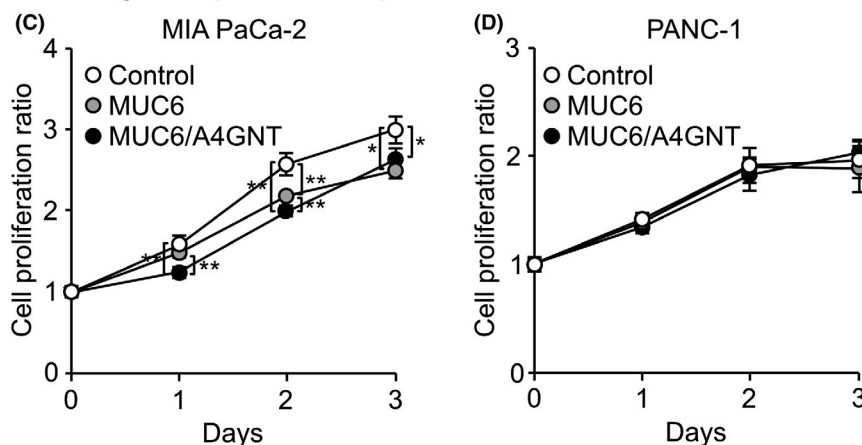
FIGURE 2 Effects of α4GnT and MUC6 expression on MIA PaCa-2 and PANC-1 cell proliferation. A, B, Anchorage-dependent proliferation analysis. MIA PaCa-2 (A) or PANC-1 (B) cells transduced as indicated were seeded at 1×10^3 cells per well in 96-well tissue culture plates, and an MTS assay was performed daily for 3 d. A cell proliferation ratio was calculated with the value on day 0 set to 1. C, D, Anchorage-independent proliferation analysis. MIA PaCa-2 (C) or PANC-1 (D) cells transduced as indicated were seeded in poly-HEMA–coated 96-well plates and assayed using the same procedure described to assess anchorage-dependent proliferation. Results are expressed as the mean (n = 6) and error bars indicate SD. Representative results from four independent experiments are shown. *P < .05 and **P < .01
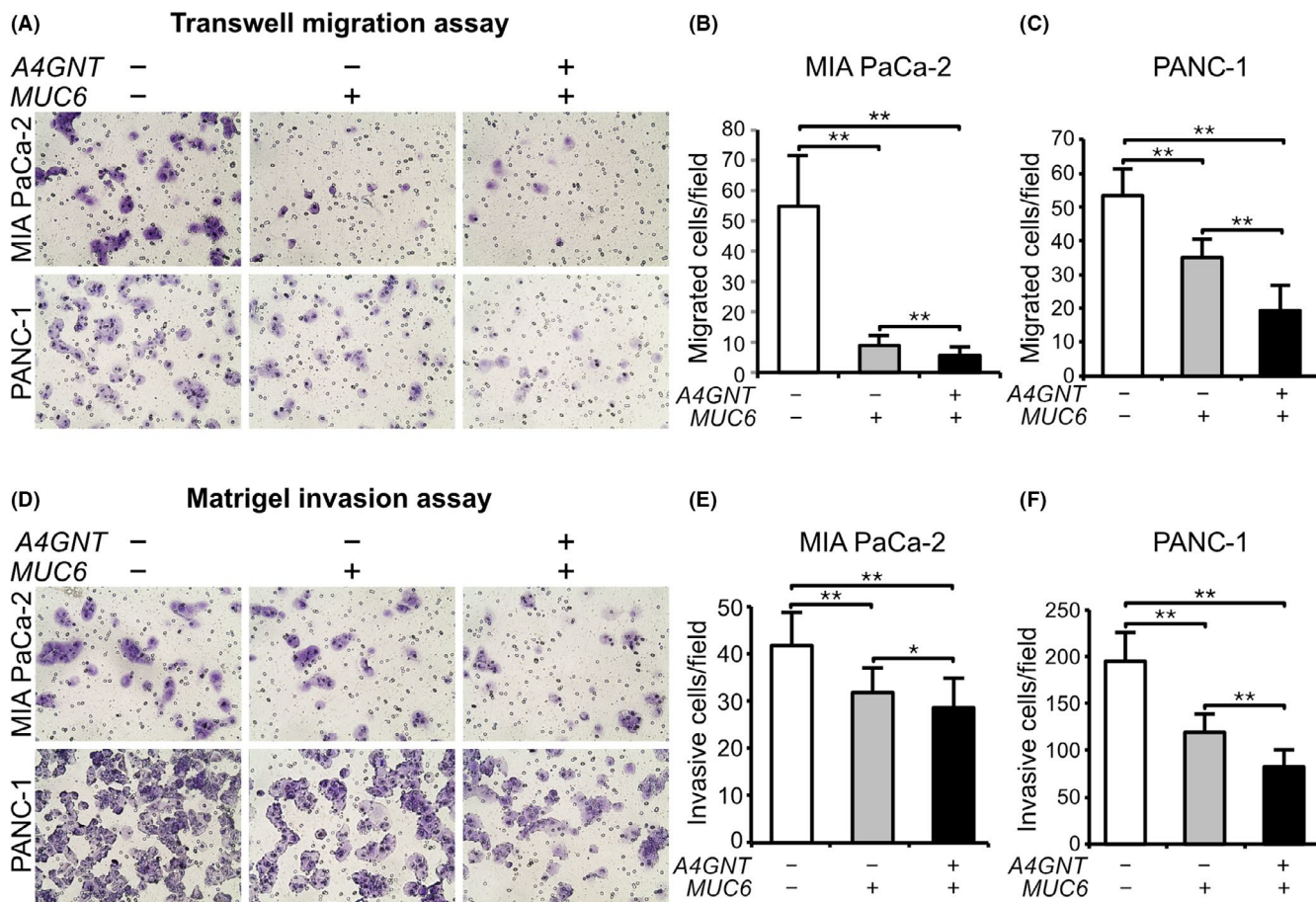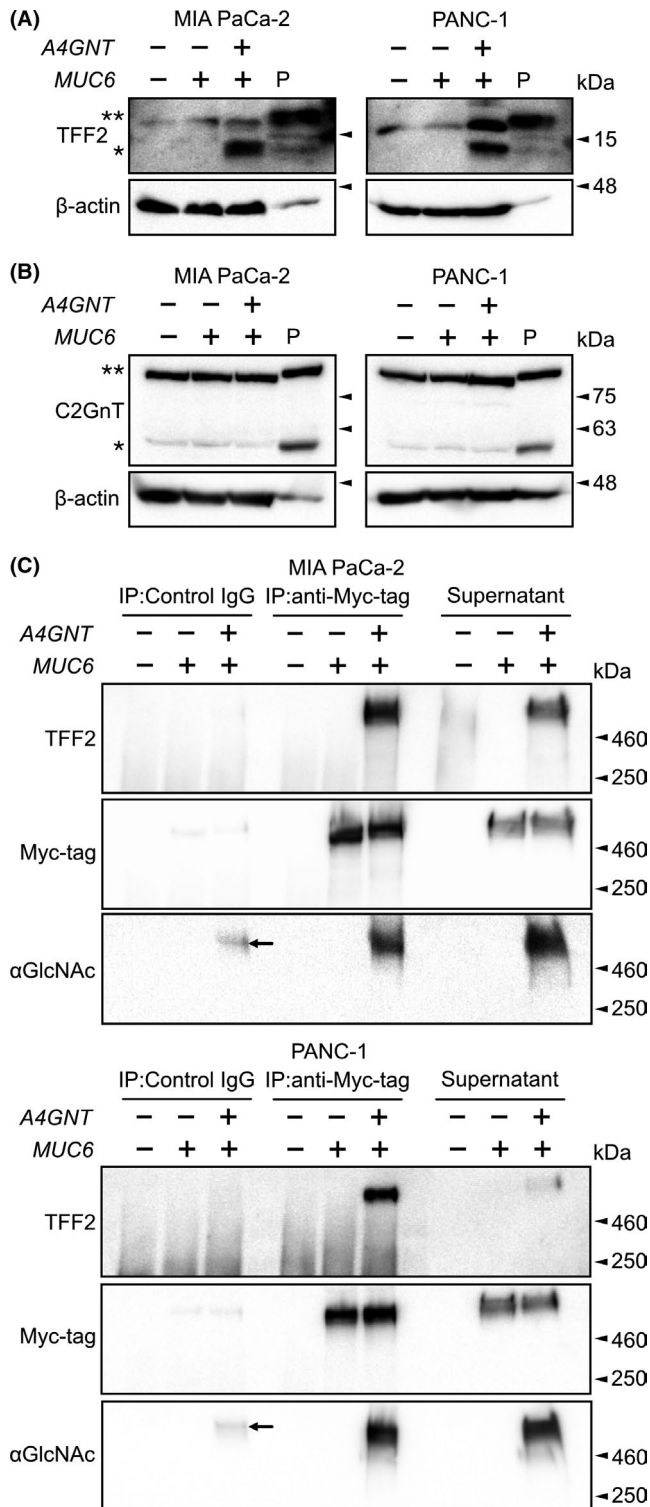
FIGURE 3 Transwell migration and Matrigel invasion assays. A-C, Transwell migration assays. A, Representative photographs of MIA PaCa-2 (upper panel) and PANC-1 (lower panel) cells transduced as indicated. B, C, Quantification of MIA PaCa-2 (B) and PANC-1 (C) cell migration. Migrated cells were observed by light microscopy ($\times$200 magnification) and counted in five randomly selected fields from triplicate wells. Results are expressed as the mean (n = 15), and error bars indicate SD. Representative results from four independent experiments are shown. **$P < .01$. D-F, Matrigel invasion assays. D, Representative photographs of MIA PaCa-2 (upper panel) and PANC-1 (lower panel) cells transduced as indicated. E, F, Quantification of MIA PaCa-2 (E) and PANC-1 (F) cell invasiveness. Invasive cells were observed by light microscopy ($\times$200 magnification) and counted in five randomly selected fields from triplicate wells. Results are expressed as the mean (n = 15) and error bars indicate SD. Representative results from four independent experiments are shown. *$P < .05$ and **$P < .01$

3.4 | Effect of ectopic MUC6 and α4GnT expression on cellular invasiveness

We next assessed effects of ectopic MUC6 and α4GnT expression on cellular invasiveness using a Matrigel invasion assay. In that analysis we observed significantly fewer invaded cells relative to controls in MIA PaCa-2-MUC6 cells (Figure 3D, E). Accordingly, MIA PaCa-2-MUC6/A4GNT cells showed significantly decreased invasiveness relative to MIA PaCa-2-MUC6 cells (Figure 3D, E). We observed comparable phenotypes of decreased invasiveness relative to controls following analysis of PANC-1-MUC6 and PANC-1-MUC6/A4GNT cells (Figure 3D, F). These results suggest that in both MIA PaCa-2 and PANC-1 cells, ectopic MUC6 expression significantly attenuates cellular invasiveness, and that glycosylation of MUC6 with αGlcNAc promotes a significantly more robust effect.

3.5 | αGlcNAc-bound MUC6 formed a complex with TFF2

In normal gastric mucosa, TFF2 binds to MUC6 through αGlcNAc to form a molecular complex that increases the viscosity of mucus.[29-32] Thus, we focused on TFF2 expression in MIA PaCa-2 and PANC-1. TFF2 was expressed in both cell lines and increased by dual expression of MUC6/α4GnT (Figure 4A). As TFF2 binds more strongly to αGlcNAc on core 2 structure than to that on core 1 structure,[30] we assessed C2GnT expression to clarify αGlcNAc-bound structure in the two cell lines. C2GnT was expressed in both cell lines (Figure 4B) indicating that αGlcNAc is on core 2 structure in MIA PaCa-2 and PANC-1. Then, we analyzed secreted MUC6 and TFF2 in the culture supernatant. Only glycosylated MUC6 was detected in the culture supernatant (Figure 4C, Myc-tag panel). When culture supernatants were immunoprecipitated with anti-Myc-tag, the products showed anti-TFF2–reactive bands above 460 kDa in both cell lines (Figure 4C,

(A)

(B)

(C)

FIGURE 4 Analysis of the αGlcNAc-bound MUC6 and TFF2 complex. A, B, Expression analysis of endogenous TFF2 (A) and C2GnT (B) in MIA PaCa-2 and PANC-1 cells. Whole-cell lysates (WCLs) of AGS cells ectopically expressing TFF2 or C2GnT were used as a positive control (P). *, unglycosylated form of TFF2 or C2GnT; **, glycosylated form of TFF2 or C2GnT. β-actin serves as the loading control. C, Immunoprecipitation (IP) and Western blotting analysis of the αGlcNAc-bound MUC6 and TFF2 complex. Culture supernatants from MIA PaCa-2 or PANC-1 cells transduced with *MUC6*, *MUC6/A4GNT*, or control, as indicated, were immunoprecipitated and immunoblotted with antibodies shown in the figure. Nonspecific bindings to beads are indicated by arrows
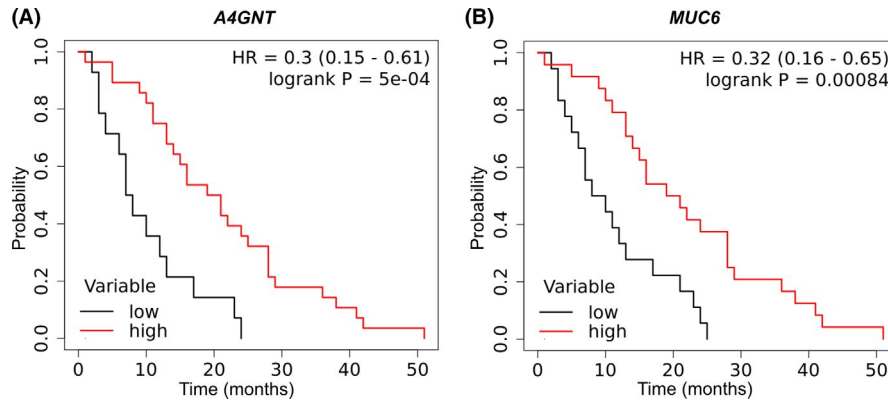
3.6 | Prognostic value of *A4GNT* and *MUC6* expression in human pancreatic ductal adenocarcinoma

Finally, we evaluated a potential correlation between *A4GNT* or *MUC6* mRNA expression and prognosis using human pancreatic ductal adenocarcinoma cases in the GEO database. To do so, we plotted survival curves relevant to pancreatic ductal adenocarcinoma patients using a Kaplan-Meier plotter. The database was based on 45 patients with pancreatic ductal adenocarcinoma, but there was no survival information for three of the 45 cases. Among the 42 cases analyzed, the population with high *A4GNT* expression (n = 28) had a significantly more favorable prognosis than the population exhibiting low expression (n = 14, HR = 0.3 [0.15-0.61], *P* = 5e-04) (Figure 5A). Moreover, the population with relatively high *MUC6* expression (n = 24) showed a significantly more preferable prognosis than the population with low expression (n = 18, HR = 0.32 [0.16-0.65], *P* = .00084) (Figure 5B). Overall, these results indicate that both *A4GNT* and *MUC6* transcript levels positively correlate with more favorable prognosis of patients with pancreatic ductal adenocarcinoma.

4 | DISCUSSION

In this study, we demonstrate that ectopic expression in pancreatic cancer MIA PaCa-2 or PANC-1 cells of MUC6, either alone or combined with α4GnT, attenuates anchorage-dependent cell proliferation, cellular motility, and cellular invasiveness in vitro. We also report that expression levels of *A4GNT* and *MUC6* transcripts, which encode α4GnT and MUC6, respectively, significantly correlated with the prognosis of pancreatic ductal adenocarcinoma patients. Both lines of evidence suggest that α4GnT and MUC6 expression in pancreatic ductal adenocarcinoma is associated with more favorable outcomes for patients.

We previously used immunohistochemistry to assess expression patterns of the gastric mucin markers MUC5AC, MUC6, and αGlcNAc in precursor lesions of pancreatic cancer as well as in invasive carcinoma.[20] That analysis revealed that αGlcNAc expression levels begin to decrease relative to MUC6 early in tumor progression in both the PanIN-IDAC and IPMN-IPMNAIC sequences.[20]

TFF2 panel). This mobility was identical to that of αGlcNAc-bound MUC6, ie, anti-Myc-tag– and anti-αGlcNAc–reactive bands (Figure 4C, Myc-tag and αGlcNAc panel). Considering that the molecular weight of TFF2 is 14-18 kDa, the detection of TFF2 at higher molecular weight indicates that it formed an SDS- and 2-mercaptoethanol–resistant complex with αGlcNAc-bound MUC6. These results suggest that MIA PaCa-2-MUC6/A4GNT and PANC-1-MUC6/A4GNT cells are surrounded by the highly viscous MUC6-TFF2 complex.

FIGURE 5 Correlation of *A4GNT* or *MUC6* expression with prognosis of patients with pancreatic cancer. A, Kaplan-Meier curves depicting survival time for patients with pancreatic ductal adenocarcinoma whose samples showed high or low *A4GNT* expression. Red line indicates cases (n = 28) with high *A4GNT* expression, and black line indicates cases (n = 14) with low *A4GNT* expression. B, Kaplan-Meier curves depicting survival time for patients with pancreatic ductal adenocarcinoma whose samples showed high or low *MUC6* expression. Red line indicates cases (n = 24) with high *MUC6* expression, and black line indicates cases (n = 18) with low *MUC6* expression. HR, hazard ratio
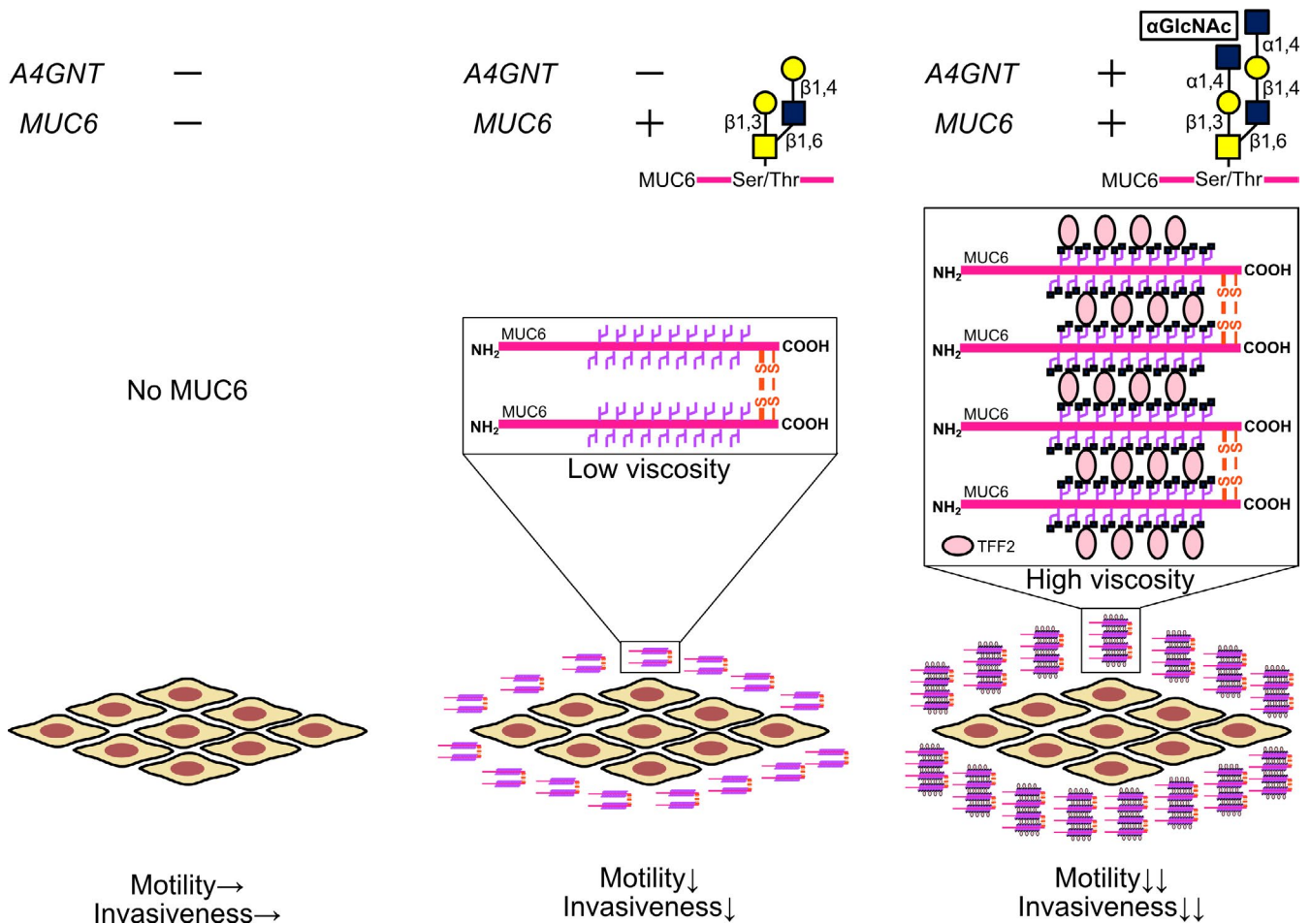
FIGURE 6 Schematic representation of the inhibitory effects of αGlcNAc and MUC6 on cellular motility and invasiveness. When MUC6 is ectopically expressed, cells are surrounded by MUC6, thus reducing motility and invasiveness. When αGlcNAc is attached to MUC6 by α4GnT, complexes of αGlcNAc-bound MUC6 and TFF2 are formed, resulting in a more potent effect because the cells are surrounded by the highly viscous MUC6-TFF2 complex. Yellow square, *N*-acetylgalactosamine (GalNAc); yellow circle, galactose (Gal); blue square, *N*-acetylglucosamine (GlcNAc)

MUC6 was also downregulated or lost in invasive stages, whereas MUC5AC was comparably expressed at all stages.[20] Moreover, decreased αGlcNAc expression relative to MUC6 occurred at early stages in malignancies of the stomach,[12,15-18] Barrett's esophagus,[18,19] uterine cervix,[21,22] biliary tract,[23] and ovary,[24] and MUC6 expression was subsequently suppressed at late stages of tumor development.[21,23,24] To investigate the function of MUC6 expression and αGlcNAc glycosylation in pancreatic cancer progression, here we ectopically expressed MUC6 or MUC6 plus α4GnT in the pancreatic cancer cell lines MIA PaCa-2 and PANC-1 and compared resultant malignant phenotypes with those seen in controls. In clinical samples of human pancreatic cancer, MUC6-negative and αGlcNAc-positive cases are rare and exceptional. In fact, we have previously reported that out of 20 cases of invasive ductal adenocarcinoma, only one case was MUC6 negative and αGlcNAc positive, and the expression level of αGlcNAc in this particular case was low.[20] Therefore, we did not analyze the cells ectopically expressing α4GnT alone. Proliferation of MIA PaCa-2 cells was attenuated by ectopic MUC6 expression and further suppressed by cotransduction with α4GnT (Figure 2A, C). Ectopic expression of both α4GnT and MUC6 also suppressed anchorage-dependent proliferation of PANC-1 cells (Figure 2B). Moreover, migration ability relative to controls of both lines was reduced by ectopic MUC6 expression and further decreased by cotransduction with α4GnT (Figure 3A-C). Furthermore, MIA PaCa-2 and PANC-1 cell invasiveness was attenuated relative to controls by ectopic MUC6 expression and further decreased by additional transduction with α4GnT in both lines (Figure 3D-F). These results strongly suggest that coexpression of MUC6 and α4GnT constructs, which likely generates MUC6 glycosylated with αGlcNAc, has a tumor-suppressive effect on cultured pancreatic cancer cells, findings that support previous pathological results.

MUC6 is highly expressed at early noninvasive stages of pancreatic tumor progression and then suppressed or lost at invasive stages.[4,6,7,20,33] Here, we demonstrated that ectopic MUC6 expression reduced invasiveness of MIA PaCa-2 and PANC-1 cells (Figure 3D-F), in agreement with the above studies. Leir et al reported that expression of MUC6 N- or C-terminal domains decreased PANC-1 cell invasion through a reconstituted matrix barrier containing collagen type IV, laminin, and gelatin by 70% or 57%, respectively, relative to vector controls.[34] Their group used the same method to assess invasiveness of colon cancer LS180 cells and breast cancer MCF7 cells. LS180 cell invasiveness was reduced by MUC6 N- or C-terminal protein expression by 41% or 46%, respectively.[34] By contrast, MCF7 cells, which are known to be poorly invasive,[35] showed <1% of invasive cells in both vector controls and MUC6 N- or C-terminal protein–expressing cells, suggesting that MUC6 alone has little effect on the behavior of poorly invasive cells.[34] These authors report that they tried to establish cells stably expressing full length of MUC6 as a minigene containing the N- and C-terminus together with the shortened tandem repeat but that cells did not proliferate in any case.[34] By contrast, we established MIA PaCa-2 and PANC-1 cells stably expressing full-length MUC6, possibly due to differences in gene transduction methods. Overall, these results indicate that MUC6 attenuates invasion of highly invasive pancreatic cancer cells.

We observed that cellular motility and invasiveness were attenuated by MUC6 transduction and further decreased by additional α4GnT expression in two cell lines (Figure 3). We also found that αGlcNAc-bound MUC6 was secreted as an SDS- and 2-mercaptoethanol–resistant complex with TFF2 from both cell lines (Figure 4C). TFF2 is reported to increase the viscosity of mucus in vitro and in vivo,[31,32] suggesting that the MUC6-TFF2 complex shows higher viscosity than free MUC6. Based on these findings, we hypothesized a mechanism of inhibitory effects of MUC6 and αGlcNAc on motility and invasiveness. When cells ectopically expressed MUC6 alone, free MUC6 surrounded the cells and inhibited motility and invasiveness (Figure 6). Furthermore, when cells additionally expressed α4GnT, αGlcNAc was synthesized on MUC6. Then, TFF2 bound to it to form a complex, resulting in the cells being surrounded by a more viscous complex, showing stronger effects (Figure 6).

We previously showed that αGlcNAc loss was significantly correlated with the depth of invasion, stage, venous invasion, and poor prognosis in MUC6-positive differentiated gastric adenocarcinoma patients.[17] We also reported that patients whose tumor samples were α4GnT and αGlcNAc positive showed significantly better prognosis than those whose samples were α4GnT and αGlcNAc negative in terms of both overall and progression-free survival in cases of uterine cervical tumors, gastric type.[22] Here, in this study, we demonstrated that higher expression of *A4GNT* mRNA was correlated significantly with favorable prognosis as compared with lower expression in pancreatic ductal adenocarcinoma patients (Figure 5A). Moreover, accumulating results indicate that MUC6-positive or higher-expressing cases showed preferable prognosis in gastric cancer,[36] colorectal cancer,[37] and pulmonary invasive mucinous adenocarcinoma.[38] We also examined *MUC6* mRNA expression and prognosis of pancreatic ductal adenocarcinoma patients and found that higher mRNA levels were significantly correlated with favorable prognosis as compared with lower levels (Figure 5B). The present study also strongly supports the idea that α4GnT and MUC6 exert tumor-suppressive effects on two pancreatic cancer cell lines and suggests that α4GnT, or αGlcNAc, and MUC6 may also be good prognostic markers in pancreatic cancer.

In conclusion, we observed attenuation of malignant phenotypes following ectopic expression of MUC6 in pancreatic cancer cell lines, effects enhanced by coexpression of α4GnT in vitro. Moreover, in patient samples, higher *A4GNT* and *MUC6* transcript levels were correlated with favorable prognosis in pancreatic ductal adenocarcinoma. We conclude that MUC6 loss and/or loss of αGlcNAc glycosylation of MUC6 could be a useful biomarker to assess pancreatic cancer progression.

CONFLICT OF INTEREST

The authors declare no conflict of interest.

ORCID

Chifumi Fujii https://orcid.org/0000-0001-8735-5274
Kazuhiro Yamanoi https://orcid.org/0000-0002-5361-8053
Masatomo Kawakubo https://orcid.org/0000-0001-5106-5742
Jun Nakayama https://orcid.org/0000-0001-6773-2802

REFERENCES

1. Sung H, Ferlay J, Siegel RL, et al. Global cancer statistics 2020: globocan estimates of incidence and mortality worldwide for 36 Cancers in 185 countries. *CA Cancer J Clin*. 2021;71:209-249.
2. Kim YS, Gum J Jr, Brockhausen I. Mucin glycoproteins in neoplasia. *Glycoconj J*. 1996;13:693-707.
3. Kim GE, Bae HI, Park HU, et al. Aberrant expression of MUC5AC and MUC6 gastric mucins and sialyl Tn antigen in intraepithelial neoplasms of the pancreas. *Gastroenterology*. 2002;123:1052-1060.
4. Prasad NB, Biankin AV, Fukushima N, et al. Gene expression profiles in pancreatic intraepithelial neoplasia reflect the effects of Hedgehog signaling on pancreatic ductal epithelial cells. *Cancer Res*. 2005;65:1619-1626.
5. Ban S, Naitoh Y, Mino-Kenudson M, et al. Intraductal papillary mucinous neoplasm (IPMN) of the pancreas: its histopathologic difference between 2 major types. *Am J Surg Pathol*. 2006;30:1561-1569.
6. Nagata K, Horinouchi M, Saitou M, et al. Mucin expression profile in pancreatic cancer and the precursor lesions. *J Hepatobiliary Pancreat Surg*. 2007;14:243-254.
7. Basturk O, Khayyata S, Klimstra DS, et al. Preferential expression of MUC6 in oncocytic and pancreatobiliary types of intraductal papillary neoplasms highlights a pyloropancreatic pathway, distinct from the intestinal pathway, in pancreatic carcinogenesis. *Am J Surg Pathol*. 2010;34:364-370.
8. Ota H, Katsuyama T, Ishii K, Nakayama J, Shiozawa T, Tsukahara Y. A dual staining method for identifying mucins of different gastric epithelial mucous cells. *Histochem J*. 1991;23:22-28.
9. Nordman H, Davies JR, Lindell G, de Bolós C, Real F, Carlstedt I. Gastric MUC5AC and MUC6 are large oligomeric mucins that differ in size, glycosylation and tissue distribution. *Biochem J*. 2002;364:191-200.
10. Ishihara K, Kurihara M, Goso Y, et al. Peripheral α-linked *N*-acetylglucosamine on the carbohydrate moiety of mucin derived from mammalian gastric gland mucous cells: epitope recognized by a newly characterized monoclonal antibody. *Biochem J*. 1996;318:409-416.
11. Zhang MX, Nakayama J, Hidaka E, et al. Immunohistochemical demonstration of α1,4-*N*-acetylglucosaminyltransferase that forms GlcNAc α1,4Galβ residues in human gastrointestinal mucosa. *J Histochem Cytochem*. 2001;49:587-596.
12. Nakayama J. Dual roles of gastric gland mucin-specific O-glycans in prevention of gastric cancer. *Acta Histochem Cytochem*. 2014;47:1-9.
13. Nakayama J, Yeh JC, Misra AK, Ito S, Katsuyama T, Fukuda M. Expression cloning of a human α1,4-*N*-acetylglucosaminyltransferase that forms GlcNAc α1→4Galβ→R, a glycan specifically expressed in the gastric gland mucous cell-type mucin. *Proc Natl Acad Sci USA*. 1999;96:8991-8996.
14. Karasawa F, Shiota A, Goso Y, et al. Essential role of gastric gland mucin in preventing gastric cancer in mice. *J Clin Invest*. 2012;122:923-934.
15. Yamada S, Okamura T, Kobayashi S, Tanaka E, Nakayama J. Reduced gland mucin-specific *O*-glycan in gastric atrophy: a possible risk factor for differentiated-type adenocarcinoma of the stomach. *J Gastroenterol Hepatol*. 2015;30:1478-1484.
16. Yamanoi K, Sekine S, Higuchi K, Kushima R, Nakayama J. Decreased expression of gastric gland mucin-specific glycan α1,4-linked *N*-acetylglucosamine on its scaffold mucin 6 is associated with malignant potential of pyloric gland adenoma of the stomach. *Histopathology*. 2015;67:898-904.
17. Shiratsu K, Higuchi K, Nakayama J. Loss of gastric gland mucin-specific O-glycan is associated with progression of differentiated-type adenocarcinoma of the stomach. *Cancer Sci*. 2014;105:126-133.
18. Yamanoi K, Nakayama J. Reduced αGlcNAc glycosylation on gastric gland mucin is a biomarker of malignant potential for gastric cancer, Barrett's adenocarcinoma, and pancreatic cancer. *Histochem Cell Biol*. 2018;149:569-575.
19. Iwaya Y, Hasebe O, Koide N, et al. Reduced expression of αGlcNAc in Barrett's oesophagus adjacent to Barrett's adenocarcinoma - a possible biomarker to predict the malignant potential of Barrett's oesophagus. *Histopathology*. 2014;64:536-546.
20. Ohya A, Yamanoi K, Shimojo H, Fujii C, Nakayama J. Gastric gland mucin-specific O-glycan expression decreases with tumor progression from precursor lesions to pancreatic cancer. *Cancer Sci*. 2017;108:1897-1902.
21. Yamanoi K, Ishii K, Tsukamoto M, Asaka S, Nakayama J. Gastric gland mucin-specific O-glycan expression decreases as tumor cells progress from lobular endocervical gland hyperplasia to cervical mucinous carcinoma, gastric type. *Virchows Arch*. 2018;473:305-311.
22. Ida K, Yamanoi K, Asaka S, et al. αGlcNAc and its catalyst α4GnT are diagnostic and prognostic markers in uterine cervical tumor, gastric type. *Sci Rep*. 2019;9:13043.
23. Okumura M, Yamanoi K, Uehara T, Nakayama J. Decreased alpha-1,4-linked *N*-acetylglucosamine glycosylation in biliary tract cancer progression from biliary intraepithelial neoplasia to invasive adenocarcinoma. *Cancer Sci*. 2020;111:4629-4635.
24. Ohya A, Matoba H, Fujinaga Y, Nakayama J. Decreased gastric gland mucin-specific *O*-glycans are involved in the progression of ovarian primary micinous tumors. *Acta Histochem Cytochem*. 2021;54:115-122.
25. Kobayashi M, Fujinaga Y, Ota H. Reappraisal of the immunophenotype of pancreatic intraductal papillary mucinous neoplasms (IPMNs)-gastric pyloric and small intestinal immunophenotype expression in gastric and intestinal type IPMNs-. *Acta Histochem Cytochem*. 2014;47:45-57.
26. Miyamoto T, Suzuki A, Asaka R, et al. Immunohistochemical expression of core 2 β1,6-N-acetylglucosaminyl transferase 1 (C2GnT1) in endometrioid-type endometrial carcinoma: a novel potential prognostic factor. *Histopathology*. 2013;62:986-993.
27. Kanda Y. Investigation of the freely available easy-to-use software 'EZR' for medical statistics. *Bone Marrow Transplant*. 2013;48:452-458.
28. Reis CA, David L, Carvalho F, et al. Immunohistochemical study of the expression of MUC6 mucin and co-expression of other secreted mucins (MUC5AC and MUC2) in human gastric carcinomas. *J Histochem Cytochem*. 2000;48:377-388.
29. Hoffmann W. TFF2, a MUC6-binding lectin stabilizing the gastric mucus barrier and more (Review). *Int J Oncol*. 2015;47:806-816.
30. Hanisch FG, Bonar D, Schloerer N, Schroten H. Human trefoil factor 2 is a lectin that binds α-GlcNAc-capped mucin glycans with antibiotic activity against Helicobacter pylori. *J Biol Chem*. 2014;289:27363-27375.
31. Thim L, Madsen F, Poulsen SS. Effect of trefoil factors on the viscoelastic properties of mucus gels. *Eur J Clin Invest*. 2002;32:519-527.
32. Kjellev S, Nexø E, Thim L, Poulsen SS. Systemically administered trefoil factors are secreted into the gastric lumen and increase the viscosity of gastric contents. *Br J Pharmacol*. 2006;149:92-99.
33. Sierzega M, Młynarski D, Tomaszewska R, Kulig J. Semiquantitative immunohistochemistry for mucin (MUC1, MUC2, MUC3, MUC4, MUC5AC, and MUC6) profiling of pancreatic ductal cell

adenocarcinoma improves diagnostic and prognostic performance. *Histopathology*. 2016;69:582-591.

34. Leir SH, Harris A. MUC6 mucin expression inhibits tumor cell invasion. *Exp Cell Res*. 2011;317:2408-2419.

35. Liu Z, Brattain MG, Appert H. Differential display of reticulocalbin in the highly invasive cell line, MDA-MB-435, versus the poorly invasive cell line, MCF-7. *Biochem Biophys Res Commun*. 1997;231:283-289.

36. Zheng H, Takahashi H, Nakajima T, et al. MUC6 down-regulation correlates with gastric carcinoma progression and a poor prognosis: an immunohistochemical study with tissue microarrays. *J Cancer Res Clin Oncol*. 2006;132:817-823.

37. Betge J, Schneider NI, Harbaum L, et al. MUC1, MUC2, MUC5AC, and MUC6 in colorectal cancer: expression profiles and clinical significance. *Virchows Arch*. 2016;469:255-265.

38. Kishikawa S, Hayashi T, Saito T, et al. Diffuse expression of MUC6 defines a distinct clinicopathological subset of pulmonary invasive mucinous adenocarcinoma. *Mod Pathol*. 2021;34:786-797.